Article

Assessment of the Use of Solar Desalination Distillers to Produce Fresh Water in Arid Areas

Joaquim Monteiro, Andresa Baptista *, Gustavo Pinto, Leonardo Ribeiro and Hélder Mariano

ISEP—School of Engineering, Polytechnic of Porto, 4200-072 Porto, Portugal; jfmo@isep.ipp.pt (J.M.); gustavopinto@eu.ipp.pt (G.P.); lsr@isep.ipp.pt (L.R.); 1101342@isep.ipp.pt (H.M.)

* Correspondence: absa@isep.ipp.pt; Tel.: +351-228-340-500

check for updates

Abstract: Water is an important resource for human beings, yet there are inhabited places tormented by the scarcity of it. The present study is concerned with places where, seemingly, the best way to get water is through solar distillers. These places should have, typically, high values of solar irradiation and a lack of human and economic resources to build and operate complex equipment. A set of sites scattered around the world was chosen, and then the presumed productivity and thermal efficiency that solar distillers would have if they were installed at these places was calculated. The mathematical model used with this purpose assumes steady state operation; the values of mass of water distilled and distiller efficiency were calculated for every hour, but the results presented are annual averages. Then, an economic study was made based on local costs of construction materials for the distillers, the work force, and the prices of water to predict the payback time of solar distillers. Finally, a study on environmental impact, particularly in terms of greenhouse gas (GHG) emissions, was made to compare reverse osmosis (RO) with solar distillation. For the sites studied, typical values of annual water output are in the range of 414 dm^3/m^2, for Évora, up to 696 dm^3/m^2, for Faya Largeau; the minimum efficiency was found for Évora, as 11.5%, and the maximum efficiency was found for Tessalit, as 15.2%. Payback times are very high, regardless of the areas of the globe where solar distillers are implanted. Regarding the GHG emissions, solar distillation is preferable to RO.

Keywords: solar desalination; distillers; fresh water; arid areas; GHG emissions

1. Introduction

1.1. Overview

Needless to say, water is of paramount importance to almost all forms of life. Some think tanks concerned with geostrategic matters have even predicted that in the near future, wars will be waged because of lack of water.

The regions of the planet already distressed by water shortage are located in vast deserts in the north of Africa, Namibia, the outback of Australia, central Asia, North and South Americas, and some tiny islands in the middle of oceans. Moreover, because of climate change such places are appearing with increasing frequency.

It is not simply water that worries human beings, since water, namely, brackish water, is abundant and widespread; what worries human beings is the scarcity of fresh water. Yet, there are several ways to get fresh water from brackish water.

Desalination through distillation is a way to obtain fresh water from brackish or salted water. There are several methods to desalinate water, grouped by the authors of [1] as thermal and non-thermal; the current paper focuses only on the solar distillers, which follow a thermal method. The reason for

this choice stems on the obvious link between water shortage and poverty, and so it seems realistic to desalinate water through simple and cheap methods, resorting to long-lasting facilities with almost no maintenance requirements, constructed with materials found locally; a solar distiller may last up to 25 years without major repairs [2].

Ultimately, a solar desalination distiller consists of a cover made of transparent material, placed over a basin filled with salted water (see Figure 1). According to Belessiotis et al. [1], the cover is normally roof-shaped, double-shaped, and symmetric, but can also be asymmetric or single sloped, and there can be two covers. Solar radiation successively crosses the cover; energy is absorbed by the water in the basin; water evaporates; and vapor rises to the underside of the cover, cooler than the upper side of the cover, condenses, and then slides, preferably without falling back into the basin, to the gutters bordering the distiller. The productivity of such installation is assessed by the mass of fresh water yielded by unit area of the distiller and unit of time.
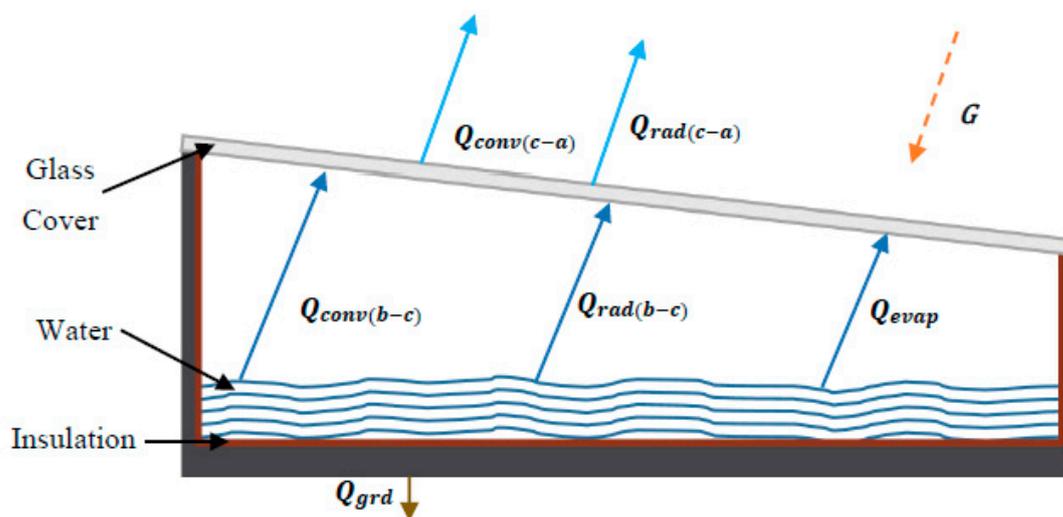

Figure 1. Schematic cross section of a typical solar distillation distiller.

The cover is usually of glass, and less often of plastic films. Glass covers have the drawback of being breakable and, according to the authors of [3], should have a hematite content lower than 0.01%. Plastic covers can be made of treated polyvinylchloride and tetraphalate-polyethylene; their durability is less than 15 years, and their adaptability to any desired shape of the distiller is the highest of their class [1]. Phadatare and Verma [4] found that the productivity of distillers covered with glass is 30% to 35% higher than the productivity for distillers covered with Plexiglas.

The slope of the cover must guarantee that the condensed droplets of water, due to their surface tension, do not fall back into the basin but slide to the gutters, to be collected; this slope is normally under 20° [2]. The gutters have a slight slope too, just enough to prompt the flow of the distilled water into a reservoir that feeds consumers of such water. If the basin is shallow, its depth ranges from 10 to 20 mm; if the basin is deep, its depth goes up to 100 mm [4]. The widths are around 2 m and the lengths can reach 100 m [4].

The floor of the basin bottom liner must be waterproof, free of toxic components, withstand temperatures up to 90 °C, have a thermal absorptivity above 0.95 (see Table 1), and a polished surface. From Belessiotis et al. [1], it is normally made of one of these materials: concrete, wood impregnated with epoxy resins, aluminum, magnesium alloys, hard plastic ultraviolet resistant as Plexiglas, etc. To increase its absorption of solar heat, the upper side of the floor of the basin is covered by one of these materials: black paint (without volatile components that could evaporate with the water), spongy materials, butyl rubber, black polyethylene, asphalt, jute, etc.

The frame that supports the glass/plastic cover has to be robust and cling to the ground to withstand inclement weather, such as sand storms, but some of its parts must be removable to allow cleaning and repairs in the distiller.

The bottom and sidewalls of the basin are insulated from the ground to lower, as much as possible, the heat losses from the distiller. The most suitable insulation materials have low conductivity, are easily applicable to this kind of basin, withstand the operation of the distiller without deformations, do not release chemicals harmful into water up to 90 °C, and are waterproof. Pumps, storage tanks, pipes, fittings, etc., are considered ancillary components. Pipes and fittings can be of the same material, such as polyvinyl chloride (PVC) or any other plastic material not damaged by temperatures up to 90 °C; pipes and fittings either of galvanized steel or copper for brackish water, and stainless steel for distilled water, can be used as well. Normally, plastic materials are cheaper than stainless steel.

The sealing between cover and basin is necessary because the volume limited by the surface of the water, the underside of the cover, and the tops of the distiller must be air tight to reduce convection losses. Good sealing materials are easily applied, non-toxic, and have very low absorptivity.

The maintenance requirements of such distillers are cheap and easy. The maintenance consists mostly in removing leaves, dust, and sand from the cover; occasionally glasses break, and then have to be replaced. Some parts must be removable to allow cleaning and repairs in the basin.

Such distillers must endure bad weather conditions, such as strong winds and sand storms.

Solar desalination distillers operate in either batch or continuous mode. In batch mode, the amount of water evaporated from the basin during one day is offset, at the next sunrise, by new salt water. To avoid scaling or algae, every two or three days the basin is emptied and then refilled with new saltwater. As the temperature of the water in the basin increases, the productivity of the distiller increases; this is the reason why during the morning and the night such productivity is low but near noon it is at a maximum. Besides, shallow basins do not store sensible heat as do deep distillers. The productivity of distilled water by shallow distillers is in phase with the value of irradiation received by the distiller and so, from sunset to sunrise, distillation stops; however, as deep distillers store heat, distillation extends after sunset, although at low rate. In continuous mode, the basin is continuously fed by saltwater in a way to keep the amount of water in the basin constant.

1.2. Sites with Distillation Distillers

There is a long record of facilities to desalinate water through solar distillation. Some of these plants are shown in in Table 1.

In 1872, such a desalination plant was built at Chacabuco, (Las Salinas, Chile), which is described in detail by the authors of [5–7]. It operated for three decades to provide drinking water for animals used in nitrate mining [5]. Additionally, at Daytona Beach (Florida, USA), a similar facility was built, operated by Battele Memorial Institute of Cleveland [8–10]. In addition, numerous studies have been published, such as that by the authors of [11–13].

The Table 2 contains some sites, scattered around the world, which are seemingly suitable to solar harnessing facilities in general. The purpose of the present work is to assess the performance of specific distillation plants eventually set up on such sites.

Table 1. Features of solar distillation plants.

Country	Sites	Construction Year	Basin Area (m^2)	Production (L/day)	Daily Production Per Area (L/m^2)	Reference
Australia	Muresk I	1963	372	833	2.24	[14–16]
	Muresk II	1966	372	833	2.24	[15–18]
	Coober Pedy	1966	3159	6359	2.01	[15]
	Caiguna	1966	372	776	2.09	[19]
	Hamelin Pool	1966	557	1211	2.17	[10,20]
	Griffith	1967	413	908	2.20	[10,20]
Cabo Verde	Santa Maria	1965	743	2120	2.85	[10,20]
Caribbean	Petit St. Vincente	1967	1709	4921	2.88	[19]
	Haiti	1969	223	757	3.39	[10,20]
Chile	Las Salinas	1872	4459	14,763	3.31	[6,21]
	Quillagua	1968	100	401	4.01	[22]
Spain	Las Marinas	1966	869	2574	2.96	[23]
USA	Daytona Beach 1	1959	228	530	2.32	[24]
	Daytona Beach 2	1959	216	379	1.75	[24,25]
	Daytona Beach 3	1961	246	568	2.31	[25]
	Daytona Beach 4	1963	149	606	4.07	[10,20]
Greece	Symi	1964	2687	7571	2.82	[26,27]
	Aegina	1965	1490	4240	2.84	[28]
	Salamis	1965	388	1098	2.83	[20]
	Patmos	1967	8640	26,119	3.02	[29,30]
	Kimolos	1968	2508	7571	3.02	[20]
	Nisiros	1969	2044	6057	2.96	[20]
India	Bhavnagar	1965	377	833	2.21	[31,32]
Mexico	California	1969	95	379	3.99	[20]
Tunisia	Chakmou	1967	439	530	1.21	[20]
	Mahdia	1968	1301	4164	3.20	[20]
USSR	Turkmenistan	1964	599	1628	2.72	[33]

Table 2. Sites studied at the present work chosen to assess their suitability to desalination through solar distillation plants.

Sites	Country	Latitude (°)	Longitude (°)	Altitude (m)	T_m Annual (°C)	G Annual (KWh m^{-2} y^{-1})
Al Fashir	Sudan	13.6	25.3	729	25.0	2482
Almeria	Spain	36.8	−2.3	21	18.7	1880
Atar	Mauritania	20.5	−13.0	231	27.0	2404
Abu Rudeis	Egypt	28.9	33.1	8	23.7	2223
Bilma	Niger	18.7	12.9	357	26.4	2428
Dakha	Western Sahara	23.7	−15.9	10	19.7	2005
Dikhil	Djibouti	11.1	42.3	490	25.3	2584
Évora	Portugal	38.5	−7.8	246	16.3	1849
Faya Largeau	Chad	17.9	19.1	235	24.4	2456
Malakal	South Sudan	9.5	31.6	394	26.7	2351
Massawa	Eritrea	15.6	39.4	10	29.3	2184
Mekele	Ethiopia	13.4	39.5	2254	16.5	2386
Mogadishu	Somalia	2.0	45.3	3	27.0	2239
Santiago	Cabo Verde	14.9	−23.5	95	24.6	2245
St. Louis	Senegal	16.0	−16.4	2.7	25.19	2174
Tessalit	Mali	20.2	0.97	494	27.8	2440

2. Analyses

The solar distillation process to obtain water was analyzed in three respects: thermal efficiency, economics, and carbon emissions.

2.1. Thermal Efficiency

Belessiotis et al., Cooper, Duffie, and Beckman [1,2,5], among others, proposed two energy equations, one for the basin and another for the cover, with almost the same terms.

In the current study, the energy equation applied to the basin is

$$G\tau_c\alpha_w - Q_{evap} - Q_{rad(b-c)} - Q_{conv(b-c)} - Q_{grd} = (Mc/A)_b \frac{dT_b}{dt}, \tag{1}$$

where the subscripts *c*, *w*, *b*, and *grd* stand for cover, water, basin, and ground, respectively; the energy equation applied to the cover, neglecting the variation of internal energy and the solar energy absorbed by it, is

$$Q_{evap} + Q_{rad(b-c)} + Q_{conv(b-c)} = Q_{conv(c-a)} + Q_{rad(c-a)}, \tag{2}$$

where the subscript *a* stands for the atmosphere. In the right-hand side of Equation (2), the sky is assumed as a plate.

Normally, for shallow and well-insulated basins, a steady-state operation can be assumed and, accordingly, the right-hand side of Equation (1) can be neglected.

According to Cooper [34], the total (all the wavelengths) and directional (angles of incidence of 0°, 30°, 45°, and 60°) values of absorptivity, transmissivity, and reflectivity for the glass cover, the water in the basin and the basin liner are given at Table 3. The angle of incidence, θ, is measured from the normal to the surface.

Dunkle [35] proposes that

$$Q_{rad(b-c)} = 0.9\sigma\left(T_b^4 - T_c^4\right), \tag{3}$$

assuming that both the water surface and the lower side surface of the cover are diffuse and gray; the value of 0.9 includes the view factor between these surfaces and their emissivities.

For the evaporation

$$Q_{evap} = 9.15 \times 10^{-7} h_c'(p_{wb} - p_{wc})h_{fg}, \tag{4}$$

with

$$h_c' = 0.884\{(T_b - T_c) + [(p_{wb} - p_{wc})/(2016 - p_{wb})]T_b\}^{1/3}, \tag{5}$$

and the mass of water evaporated per unit of time is

$$\dot{M}_{evap} = 9.15 \times 10^{-7} h'_c (p_{wb} - p_{wc}). \tag{6}$$

For the convection between the basin and the lower side surface of the cover

$$Q_{conv(b-c)} = h'_c (T_b - T_c). \tag{7}$$

For the convection between the upper surface of the cover and the atmosphere, which is normally a mixture of free and forced convection, McAdams recommends to adopt the convection coefficient as the maximum between 5 $Wm^{-2}K^{-1}$ and the value obtained with $8.6V^{0.6}L_c^{-0.4}$; so

$$h_{(c-a)} = max.\left[5;\ 8.6V^{0.6}L_c^{-0.4}\right], \tag{8}$$

with V representing the velocity of wind, expressed in meters per second, and the characteristic length, L_c, representing the cube root of the volume of the distiller, expressed in meters. Then

$$Q_{conv(c-a)} = h_{(c-a)}(T_c - T_a). \tag{9}$$

The radiation exchange between the upper face of the cover and the sky is

$$Q_{rad(c-a)} = \varepsilon_c \sigma \left(T_c^4 - T_{sk}^4\right). \tag{10}$$

The temperature of the sky was obtained by

$$T_{sk} = T_a \left[0.711 + 0.0056 T_{wb} + 0.000073 T_{wb}^2 + 0.013 \cos(15t)\right]^2. \tag{11}$$

The value of Q_{grd} is negligible, since it depends on the construction quality of the basin, which can be controlled by the builder of the basin; a well-insulated basin is usually assumed.

The performance of the distiller was assessed through the efficiency calculated with

$$\eta = \dot{M}_{evap}/G. \tag{12}$$

2.2. Economics

In order to carry out the feasibility study of a project, it is very important to make an economic analysis of it. Firstly, this requires predicting expenditures (investments, costs, and expenses) and revenues and, secondly, the analysis of some economic indicators (TCO, NPV, IRR, and payback period). The presently studied facilities consist of distillers with an area arbitrarily set as 1 m^2, and therefore the costs considered are per square meter of installation. Costs of components were obtained through the CYPE, a price generator digital platform [36].

Total cost of ownership (TCO) is a financial estimate designed to evaluate direct and indirect costs related to purchase and capital expenditures (CAPEX), in addition to operating and maintenance costs (OPEX), and can be expressed through

$$TCO = CAPEX + OPEX. \tag{13}$$

CAPEX covers only the cost of building the equipment. OPEX includes maintenance and operating costs, considering an annual inflation rate of 2% [37,38].

Considering that the equipment has a lifespan of 20 years, the cost of water per 1 m^3 is given by

$$\frac{cost}{m^3} = TCO/\left(M_{evap\text{-}yearly} \times n\right), \tag{14}$$

with n representing the operation years and $M_{evap\text{-}yearly}$ representing the mass of fresh water obtained yearly.

The net present value (*NPV*) is the balance of all cash inflows and outflows over the estimated useful life of a project, updated to the present moment, considering an inflation rate for the stipulated period. NPV can be calculated using

$$NPV = \sum_{n=0}^{n} Fa_n R_n - \sum_{n=0}^{n} Fa_n G_n, \tag{15}$$

where Fa_n is the update factor for period *n*, R_n the revenue for period *n*, and G_n the expenditure for period *n*.

The value of Fa_n is calculated through

$$Fa_n = \frac{1}{(1+i)^n}, \tag{16}$$

where *i* is the inflation rate and *n* the years of operation.

The internal rate of return (IRR) represents the return on an investment, expressed as a percentage rate. The IRR can be viewed as the rate required for *NPV* to be zero, and calculated by

$$NPV = 0 = \text{Initial Investment} + \sum_{t=1}^{n} \frac{F_n}{(1+IRR)^n}, \tag{17}$$

where F_n is the cash flow for period *n*.

The payback period represents the time it will take a project to generate returns that equal the investment, and can be calculated using

$$Payback = \frac{Investment}{Revenue/year}. \tag{18}$$

Table 3. Total and directional values of absorptivity, transmissivity, and reflectivity for the glass cover, the water in the basin, and the basin liner; these values are presented in % [34].

Angle of Incidence, θ	0°	30°	45°	60°
Glass cover				
Absorptivity, α	5	5	5	5
Transmissivity, τ	90	90	89	85
Reflectivity, ρ	5	5	6	10
Water in the basin				
Absorptivity, α	30	30	30	30
Transmissivity, τ	68	68	67	64
Reflectivity, ρ	2	2	3	6
Basin bottom (liner)				
Absorptivity, α	95	95	95	95
Transmissivity, τ	0	0	0	0
Reflectivity, ρ	5	5	5	5

2.3. Carbon Emissions

The parameter analyzed was the CO_{2e} emissions, defined by IEA 2018, corresponding to the production of 1 m^3 of fresh water. This parameter only encompasses the CO_{2e} produced by the operation of getting fresh water. Two alternative scenarios were studied: (i) the production of water through reverse osmosis (RO), currently the most widespread desalination process [39], and (ii) the production of water through solar distillation, the process presently studied. Obviously, RO consumes

electric energy unlike solar distillation. Other methods to get fresh water were excluded from this analysis due to their technical complexities or operational costs, which renders them inappropriate for small and poor communities, the main target of this study.

Table 4 contains values of total emissions of CO_{2e} and of the total electricity produced by the countries, where the sites studied are located. Specific emissions of CO_{2e} were calculated with both these values; these specific emissions depend on the energy mix of the country. Whenever there were no reliable values either of CO_{2e} emissions or the amount of electricity generated, counterpart values of the nearest country were assumed, such as in the cases of Atar, Dikhil, and Faya Largeau.

Table 4. Emissions of CO_{2e}.

Sites	CO_{2e} Emissions (Mton)	Electricity Generated (TWh)	Specific Emissions of CO_{2e} $kg_{CO_{2e}}$/kWh	Ref.
Al Fashir	6.2	15.5	0.400	[41]
Almeria	66.7	273.4	0.243	[41]
Atar	-	-	0.625 [1]	-
Abu Rudeis	89.3	188.2	0.474	[41]
Bilma	0.5	0.6	0.833	[41]
Dakha	21.6	32.8	0.658	[41]
Dikhil	-	-	1.000 [2]	-
Évora	18.1	57.7	0.314	[41]
Faya Largeau	-	-	0.400 [3]	-
Malakal	0.5	0.5	1.000	[41]
Massawa	0.4	0.4	1.000	[41]
Mekele	0	13.9	0	[41]
Mogadishu	-	-	1.000 [2]	-
Santiago	0.2	0.4	0.490	[40]
St. Louis	3.0	4.8	0.625	[41]
Tessalit	-	-	0.625 [1]	-

[1] Value from Senegal, [2] value from Eritrea, and [3] value from Sudan.

Besides, in Cabo Verde, in the year of 2018 [40], the consumption of electricity to obtain potable water through RO was 3.909 kWh/m^3 (31,684,028 kWh to get 8,106,322 m^3 of potable water); it is plausible to assume this same value for other countries, whenever RO is concerned.

3. Results

3.1. Thermal Efficiency

Results concerning output were obtained for the locations indicated at Table 2, with climatic data drawn from reference [42], equations (1) and (2), and the assumption of steady state operation for the basin and the cover.

Hourly values of Q_{evap}, $\dot{M}_{evap}$, $Q_{conv(b-c)}$, $h_{(c-a)}$, $Q_{conv(c-a)}$, and $Q_{rad(c-a)}$ were calculated with hourly values of V, T_a, T_{sk}, and T_{wb} drawn from the referred climatic site and with the above-mentioned equations, from (1) to (11). The values of absorptivity of water, transmissivity, and reflexivity of the glass cover were assumed as the averages of the homologous values contained at Table 3. The unknowns were the temperature of the basin, T_b, and the temperature of the cover, T_c, determined by a solver for nonlinear equations. Lastly, hourly values of the efficiency of the solar distiller, η, were obtained as well. Annual values shown in the following graphs were calculated with the counterpart hourly values.

Figure 2 shows the annual output of distilled water for the sites studied, whereas Figure 3 shows the annual efficiency of solar distillation plants for the same sites.
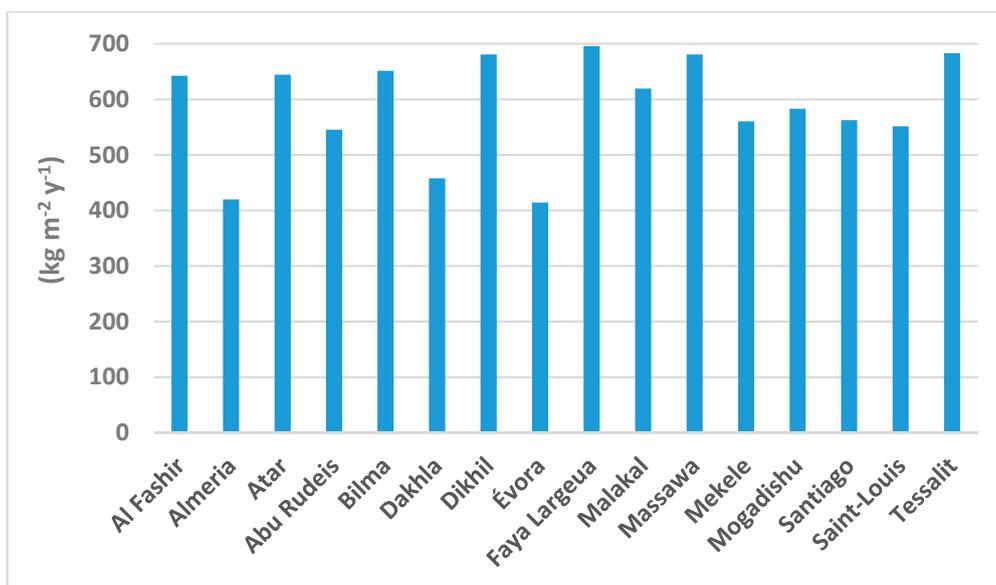
Figure 2. Annual output of distilled water for the sites studied.
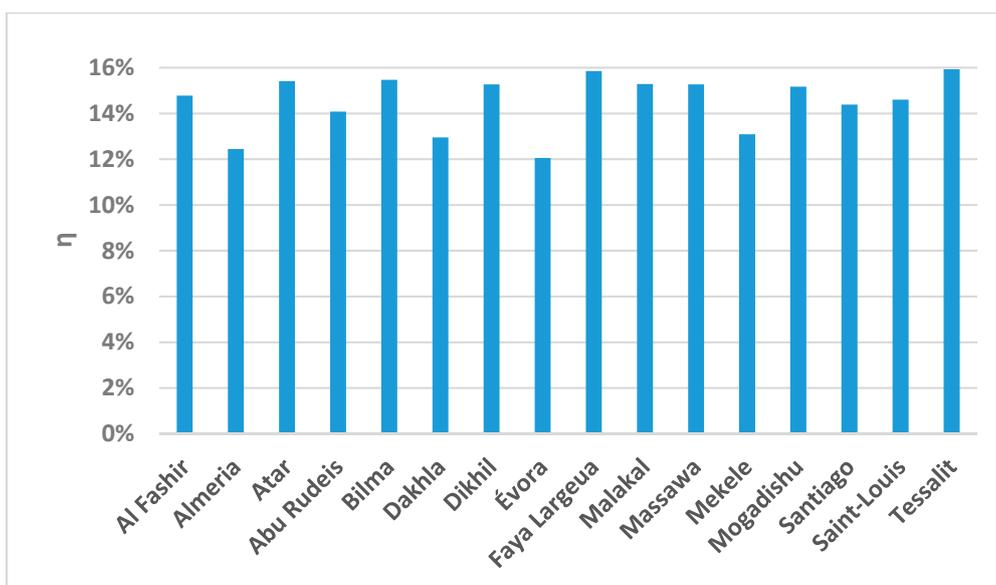

Figure 3. Efficiency of solar distillation plants for the sites studied, calculated with annual weather values.

Among the chosen sites of Table 2, the most and the least suitable for setting up solar distillation plants are, respectively, Faya Largeua and Évora. For both these sites, Figure 4 shows the monthly output of water and includes the monthly average air temperature, whereas Figure 5 shows the monthly output of water and includes the monthly average value of *G*.
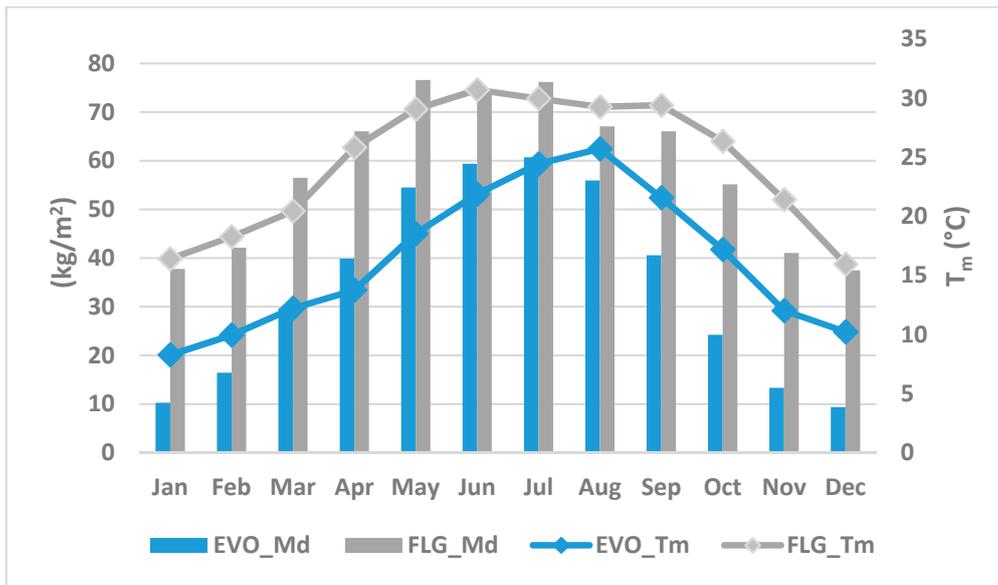
Figure 4. Monthly output of distilled water for Faya Largeua and Évora and the corresponding monthly average air temperature.
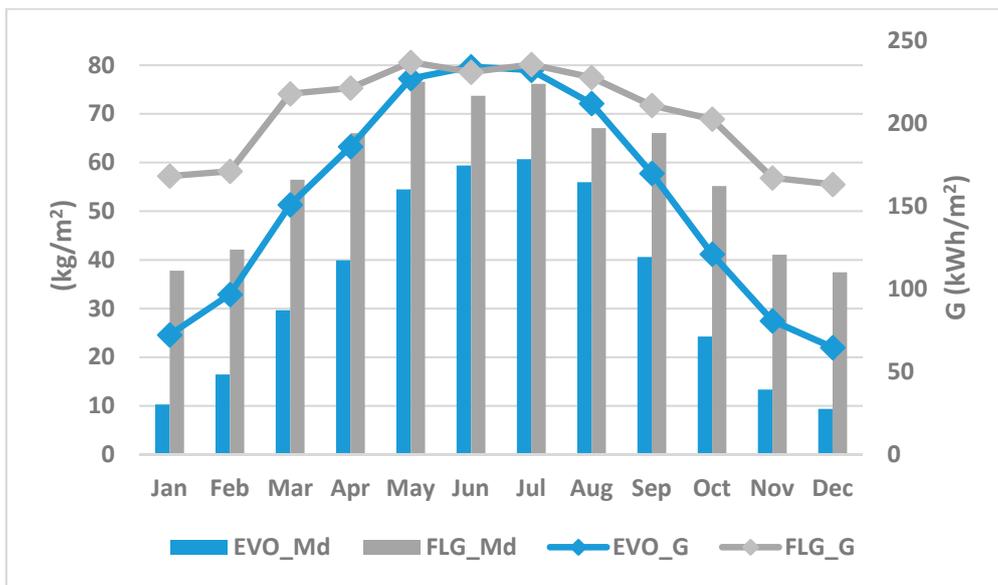

Figure 5. Annual output of distilled water for Faya Largeua and Évora and the corresponding monthly average value of *G*.

Figure 6 shows for the site with the highest water output, Faya Largeua, the monthly values of water output for two different situations: the minimum value and the actual value of the convection coefficient $h_{(c-a)}$ (see Equation (8)).

It is clear from previous figures that the productivity and the efficiency of solar distillers are higher for higher values of either irradiation *G* or average temperature T_m. Besides, the productivity and the efficiency of solar distillers increase as the convection coefficient $h_{(c-a)}$ drops. Generally, for the sites studied, when $h_{(c-a)}$ drops from the actual to the minimum value, the increase of productivity is around 10%: for the case of Faya Largeua, such an increase is 12.3%. Thus, some expedients should be

adopted to decrease, or even eliminate, the velocity of the wind over the distillers. Such expedients can be hedgerows, concrete barriers, etc.
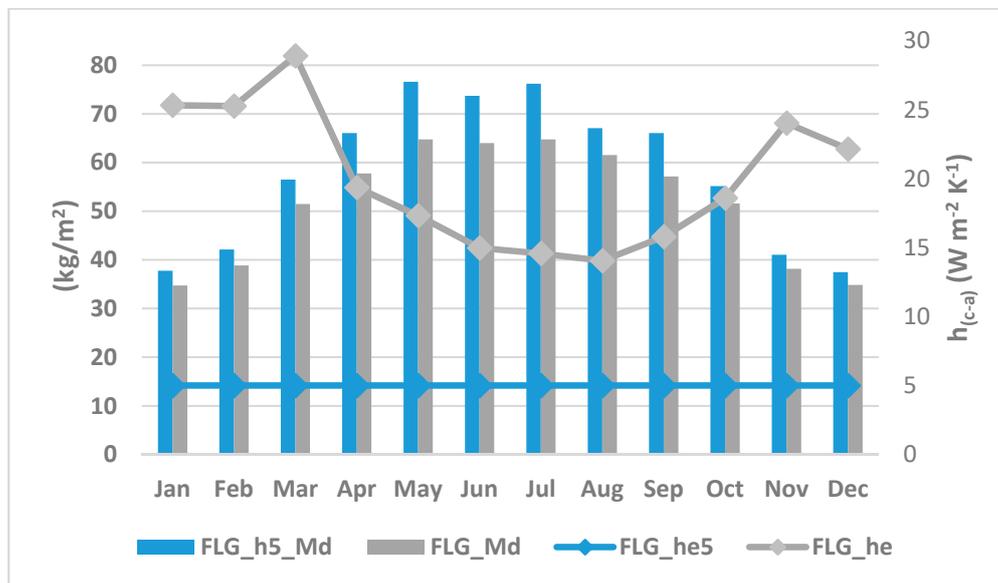

Figure 6. Comparison of the monthly output of distilled water for Faya Largeua with $h_{(c-a)} = 5$ W/m^2/K and $h_{(c-a)}$ obtained with the local wind speed measured.

3.2. Economics

An economic analysis was made for the sites referred to in Table 2, with the more important results presented in Table 5. The water annual production was drawn from Figure 2. The average costs of water for consumers were obtained from potable water suppliers: TCO, NPV for twenty years, IRR, and payback result, respectively, from Equation (12), Equation (14), Equation (16), and Equation (17).

It is important to stress that the costs of water presented in Table 5 are subsidized by the abovementioned governments.

Values of Table 5 are, at least, discouraging for poor communities of the Third World tormented by a lack of drinkable water.

Clearly, water can be obtained with distillers made with cheap materials found locally and by local unskilled people; such distillers will be affordable by poor communities, but their performance will be poor. Meanwhile, the performance and economic analyses of such distillers are impossible to calculate because (i) there is an enormous array of materials more or less suitable for the construction of distillers, and consequently, more or less expensive, and (ii) the unskillfulness of people is disputable.

So, the results presented in Table 5, however discouraging, were obtained with the underlying scope to obtain distiller with the highest efficiency, manufactured with prices current at Cabo Verde.

Anyway, from the values of payback of Table 5, it is clear that solar distillers are only suitable for domestic water production where other production methods are unavailable.

Table 5. Economic analysis summary.

Location	Average Cost of Water (€/m³)	Water Annual Production (L/m²)	*TCO* 20 Years (€/m²)	*NPV* 20 Years (€/m²)	*IRR* (%)	Payback (Years)
Al Fashir	0.766 [1]	642.6		−234.40	-	369
Almeria	0.699 [43]	420.1		−247.30	-	619
Atar	5.952 [2] [44]	644.4		−177.85	−22.1	47
Abu Rudeis	0.167 [45]	545.4		−251.27	-	1996
Bilma	0.218 [46]	651.4		−250.27	-	1280
Dakha	0.460 [47]	457.9		−248.65	-	810
Dikhil	0.448 [48]	680.9		−247.07	-	596
Évora	0.507 [49]	414.4	270.1	−248.93	-	865
Faya Largeau	0.766 [50]	695.8		−242.60	-	341
Malakal	0.766 [1]	619.4		−243.75	-	383
Massawa	0.448 [3]	680.9		−247.07	-	596
Mekele	0.448 [3]	560.5		−248.13	-	724
Mogadishu	0.448 [3]	583.0		−247.93	-	696
Santiago	4.23 [4] [40]	562.5		−206.40	-	76
St. Louis	5.952 [5]	551.6		−188.67	-	55
Tessalit	0.207 [51]	683.0		−250.28	-	1286

[1] Cost from Chad, [2] supply in 200 L drums, [3] cost from Djibouti, [4] auto tank supply, [5] and cost from Mauritania.

3.3. Carbon Emissions

Table 6 contains, for the set of sites studied, the values of Greenhouse Gas (GHG) that would be emitted if the production of the water, instead of being through the solar distillers proposed in this study, was by RO. It is considered that the operation of solar distillers does not emit GHG. The water annual production was drawn from Figure 2, and the consumption of electricity to obtain potable water through RO was assumed 3909 kWh/m³, the same as in Cabo Verde.

Table 6. Carbon emissions analysis summary.

Location	Water Annual Production (L/m²)	*RO* Desalinization Energy Consumption (kWh/m³)	*GHG* Avoid 20 Years (kg$_{CO_{2e}}$/m²)
Al Fashir	642.6		20.1
Almeria	420.1		8.0
Atar	644.4		31.5
Abu Rudeis	545.4		20.2
Bilma	651.4		42.4
Dakha	457.9		23.6
Dikhil	680.9		53.2
Évora	414.4		10.2
Faya Largeau	695.8	3909	21.8
Malakal	619.4		48.4
Massawa	680.9		53.2
Mekele	560.5		0
Mogadishu	583.0		45.6
Santiago	562.5		21.5
St. Louis	551.6		27.0
Tessalit	683.0		33.4

Clearly the environmental impact of RO is a drawback of this process when compared with solar distillation.

4. Conclusions

The scarcity of water is a problem of a growing number of regions of the world, which cumulatively are the poorest regions. Solar distillation has higher efficiency as irradiation increases and thermal losses decrease, which means that it is an acceptable desalination process for arid and hot climates.

Typical values of annual water output are in the range of 414 dm^3/m^2 for Évora and up to 696 dm^3/m^2 for Faya Largeau; the minimum efficiency found for Évora was 11.5%, and the maximum efficiency found for Tessalit was 15.2%.

However, the payback times for high performance solar distillers are very high, which excludes solar distillation when economic criteria are the only factors to be considered.

Solar distillation is far better than RO, when the environmental impact of GHG is considered. For remote and poor communities, solar distillation is to be considered.

So, as guidelines to decide if solar distillation to obtain fresh water it is important to get positive answers to the following questions:

- Remote places;
- Salt water available;
- High solar irradiation;
- Population with low income;
- Population with poor skills;
- Off-grid places.

Finally, the present study addresses the shortage of fresh water in the growing number of places that comply with the previous guidelines.

Author Contributions: The authors have made equivalent contributions. All authors have read and agreed to the published version of the manuscript.

Abbreviations

List of Symbols

A	Area of the basin	m^2
CO_{2e}	Carbon dioxide equivalent emissions	
c	Specific heat	$J\,kg^{-1}\,K^{-1}$
$CAPEX$	Capital expenditure	€
F	Casflow	€
G	SolaIrradiation	$W\,m^{-2}$
GHG	Grehouse gas	
i	Inflion rate	%
IRR	Internal rate of return	%
h	Convection coefficient	$W\,m^{-2}\,K^{-1}$
h_{fg}	Latent heat of evaporation	$J\,kg^{-1}$
Lc	Characteristic length	m
M	Mass	kg
$\dot{M}$	Mass flow rate	$kg\,s^{-1}$
NPV	Net Present Value	€
n	Period	year
$OPEX$	Operational Expenditure	€

p	Pressure	mmHg
PB	Payback	year
PVC	Polyvinyl chloride	
Q	Heat rate	W m^{-2}
R	Revenue	€
RO	Reverse osmosis	
T	Temperature	K
t	Time	s
TCO	Total cost of ownership	€
V	Wind velocity	m s^{-1}

Subscripts

a	Atmosphere	
b	Basin	
c	Cover	
conv	Convection	
d	Distilled	
evap	Evaporation	
grd	Ground	
m	Average	
n	Period	year
rad	Radiation	
sk	Sky	
w	Water	
wb	Wet bulb	

Greek symbols

α	Absorptivity	
η	Performance	
θ	Angle of incidence	
ρ	Reflectivity	
σ	Stefan-Boltzmann constant	J m^{-2} s^{-1} K^{-4}
τ	Transmissivity	

References

1. Belessiotis, V.; Kalogirou, S.; Delyannis, E. *Thermal Solar Desalination: Methods and Systems*, 1st ed.; Academic Press: Cambridge, MA, USA, 2016.
2. Cooper, P.I. The absorption of radiation in solar stills. *Sol. Energy* **1969**, *12*, 333–349. [CrossRef]
3. Kumar, K.V.; Bai, R.K. Performance study on solar still with enhanced condensation. *Desalination* **2008**, *230*, 51–61. [CrossRef]
4. Phadatare, M.K.; Verma, S.K. Effect of cover materials on heat and mass transfer coefficients in a plastic solar still. *Desalin. Water Treat.* **2009**, *2*, 254–259. [CrossRef]
5. Duffie, J.A.; Beckman, W.A. *Solar Engineering of Thermal Processes*, 4th ed.; John Wiley & Sons, Inc.: Hoboken, NJ, USA, 2013.
6. Harding, J. Apparatus for solar distillation. *Minutes Proc. Inst. Civ. Eng.* **1883**, *73*, 284–288. [CrossRef]
7. Telkes, M. Fresh water from sea water by solar distillation. *Ind. Eng. Chem.* **1953**, *45*, 1108–1114. [CrossRef]
8. Lof, G.O.G.; Eibling, J.A.; Bloemer, J.W. Energy balances in solar distillers. *AIChE J.* **1961**, *7*, 641–649. [CrossRef]
9. Bloemer, J.W.; Eibling, J.A.; Irwin, J.R. A practical basin-type solar still. *Sol. Energy* **1965**, *9*, 197–200. [CrossRef]
10. Talbert, S.G.; Eibling, J.A. *Manual on Solar Distillation of Saline Water*; NTIS: Springfield, VA, USA, 1970.
11. Hull, J.R. Solar ponds using ammonium salts. *Sol. Energy* **1986**, *36*, 551–558. [CrossRef]
12. Hull, J.R.; Bushnell, D.L.; Sempsrote, D.G.; Pena, A. Ammonium sulfate solar pond: Observations from small-scale experiments. *Sol. Energy* **1989**, *43*, 57–64. [CrossRef]

13. Nielsen, C.E. Salinity-gradient solar ponds. In *Advances in Solar Energy*; Böer, K.W., Ed.; Springer: Boston, MA, USA, 1988; Volume 4.

14. Morse, R.N. *The Development of a Solar Still for Australian Conditions*; Institution of Engineers: Barton, Australia, 1967.

15. Morse, R.N. The construction and installation of solar stills in Australia. *Desalination* **1968**, *5*, 82–89. [CrossRef]

16. Morse, R.N.; Read, W.R.W. A rational basis for the engineering development of a solar still. *Sol. Energy* **1968**, *12*, 5–17. [CrossRef]

17. Morse, R.N.; Read, W.R.W.; Trayford, R.S. Operating experiences with solar stills for water supply in Australia. *Sol. Energy* **1970**, *13*, 99–103. [CrossRef]

18. Morse, R.N. The theory of solar still operation. In Proceedings of the UN Solar Distillation Panel Meeting, Palo Alto, CA, USA, 20–23 October 1968.

19. Lawand, T. Engineering and economic evaluation of solar distillation for small communities. Presented at the Annual ASME Meeting, Los Angeles, CA, USA, 16–20 November 1969.

20. Lawand, T. Systems for solar distillation. In Proceedings of the Appropriate Technologies for Semiarid Areas: Wind and Solar Energy for Water Supply, Berlin, Germany, 15–20 September 1975.

21. Telkes, M. *Solar Stills*; Proceedings World Symposium on Applied Solar Energy: Phoenix, AZ, USA, 1956.

22. Hirschmann, J. Evaporación solar y su aplicación práctica en Chile. *Scientia* **1968**, *136*, 16.

23. Lof, G.O.G.; Hunter, J.A.; Sieder, E.N. Technical Cooperation on the Solar Distillation Development Program of Spain. In *Distillation Digest*; Tomalin, P.G., Ed.; Office of Saline Water: Washington, DC, USA, 1970; Volume 1–2, pp. 241–252.

24. Bloemer, J.W.; Collins, R.A.; Eibling, J.A. *Study and Field Evaluation of Solar Sea-Water Stills*; United States. Department of Commerce. Office of Technical Services: Washington, DC, USA, 1961.

25. Bloemer, J.W.; Irwin, J.R.; Eibling, J.A. *'Second Two-Years' Progress on Study and Field Evaluation of Solar Sea-Water Stills*; Battelle Memorial Institute: Columbus, OH, USA, 1964.

26. Eckstrom, R. Design and construction of the Symi still. *Sun Work* **1965**, *10*, 6–8.

27. Delyannis, A. Solar stills provide an island's inhabitants with water. *Sun Work* **1965**, *10*, 6.

28. Eckstrom, R. New solar stills on Greek islands. *Sun Work* **1966**, *11*.

29. Delyannis, A.; Delyannis, E.; Piperoglou, E. Solar distillation developments in Greece. *Sun Work* **1967**, *12*.

30. Delyannis, A.; Piperoglou, E. The Patmos solar distillation plant. *Sol. Energy* **1968**, *12*, 113–115. [CrossRef]

31. Datta, R.L.; Gomkale, S.D.; Ahmed, S.Y.; Datar, D.S.; Intensity, T.X.S.R. Evaporation of sea water in solar stills and its development for. In Proceedings of the First International Symposium on Water Desalination, Washington, DC, USA, 3–9 October 1965; Volume 2, p. 193.

32. Ahmed, S.Y.; Gomkale, S.D.; Datta, R.L.; Datar, D.S. Scope and development of solar stills for water desalination in India. *Desalination* **1968**, *5*, 64–74. [CrossRef]

33. Baum, V.A.; Bairamov, R. Prospects of solar stills in Turkmenia. *Sol. Energy* **1966**, *10–11*, 38–40. [CrossRef]

34. Cooper, P.I.; Bairamov, R. The maximum efficiency of single-effect solar stills. *Sol. Energy* **1973**, *15*, 205–217. [CrossRef]

35. Dunkle, R.V. Solar water distillation: The roof type still and a multiple effect diffusion still. In Proceedings of the International Heat Transfer Conference, Boulder, CO, USA, 28 August–1 September 1961; Volume 5, p. 895.

36. Gerador de Preços Para Construção Civil. Cabo Verde. CYPE Ingenieros, S.A. Available online: http://www.caboverde.geradordeprecos.info/ (accessed on 17 July 2019).

37. Chad: Inflation Rate from 1984 to 2024. Available online: https://www.statista.com/statistics/529342/inflation-rate-in-chad/ (accessed on 20 July 2019).

38. Portugal: Inflation Rate from 1984 to 2024. Available online: https://www.statista.com/statistics/529342/inflation-rate-in-portugal/ (accessed on 20 July 2019).

39. Al-Karaghouli, A.; Kazmerski, L.L. Energy consumption and water production cost of conventional and renewable-energy-powered desalination processes. *Renew. Sustain. Energy Rev.* **2013**, *24*, 343–356. [CrossRef]

40. Relatório e Contas 2018. Available online: http://www.electra.cv/index.php/2014-05-20-15-47-04/relatorios-sarl/ (accessed on 20 October 2019).

41. CO_2 Emissions from Fuel Combustion 2018 (with 2016 Data). Available online: https://webstore.iea.org/co2-emissions-from-fuel-combustion-2018 (accessed on 20 October 2019).

42. Repository of Free Climate Data for Building Performance Simulation. Available online: http://climate.onebuilding.org/ (accessed on 15 July 2019).

43. Tarifas de Abastecimiento Almeria. Available online: https://www.aqualia.com/documents/373313/374060/Almer%C3%ADa_TARIFAS+ABASTECIMIENTO.pdf/d9a04334-9c2a-425c-924d-4866c7a10802/ (accessed on 17 October 2019).

44. La Distribution d'eau Potable Dans la Ville de Nouakchott, Mauritanie. Analyse des Points de Vente d'eau. Available online: https://www.pseau.org/outils/ouvrages/gret_distribution_eau_potable_ville_nouakchott_analyse_points_d_eau.pdf (accessed on 17 October 2019).

45. Global Water Intelligence. Available online: https://www.globalwaterintel.com/news/2017/31/egypt-to-slash-subsidies-in-water-and-wastewater?dm_i=36G3,IGWK,2MX9NG,1XJV0,1 (accessed on 17 October 2019).

46. SEEN. Available online: https://www.seen-niger.com/fr/activites/relation-clientele/nos-tarifs (accessed on 17 October 2019).

47. Chohin-Kuper, A.; Strosser, P. Water pricing in Europe and around the Mediterranean Sea: Issues and options. Presented at 4th EWA Brussels Conference, Brussels, Belgium, 8 November 2008.

48. NIPA—National Investment Promotion Agency. Available online: http://www.djiboutinvest.com/index.php?option=com_content&view=article&id=289&Itemid= (accessed on 17 October 2019).

49. Tarifário dos Serviços de Abastecimento de Águas, Saneamento de Águas Residuais e Gestão de Resíduos Urbanos do Município de Évora. 2019. Available online: http://www.cm-evora.pt/pt/servicos/aguas/Paginas/Tarif%C3%A1rios.aspx (accessed on 17 October 2019).

50. UNHabitat. Available online: http://unhabitat.org/wpcontent/uploads/2015/12/Soci%C3%A9t%C3%A9%20Tchadienne%20des%20Eaux%20(Chad).pdf (accessed on 17 October 2019).

51. Fixation des Tarifs de L'Eau Potable Applicables. Available online: http://www.creemali.ml/documents/TARIFS_EAU_2013.pdf (accessed on 17 October 2019).